Equilibrium, kinetics and process design of acid yellow 132 adsorption onto red pine sawdust

Mustafa Can

ABSTRACT

Linear and non-linear regression procedures have been applied to the Langmuir, Freundlich, Tempkin, Dubinin–Radushkevich, and Redlich–Peterson isotherms for adsorption of acid yellow 132 (AY132) dye onto red pine (*Pinus resinosa*) sawdust. The effects of parameters such as particle size, stirring rate, contact time, dye concentration, adsorption dose, pH, and temperature were investigated, and interaction was characterized by Fourier transform infrared spectroscopy and field emission scanning electron microscope. The non-linear method of the Langmuir isotherm equation was found to be the best fitting model to the equilibrium data. The maximum monolayer adsorption capacity was found as 79.5 mg/g. The calculated thermodynamic results suggested that AY132 adsorption onto red pine sawdust was an exothermic, physisorption, and spontaneous process. Kinetics was analyzed by four different kinetic equations using non-linear regression analysis. The pseudo-second-order equation provides the best fit with experimental data.

Key words | acid yellow 132, batch adsorber design, isotherm, kinetic, sawdust, thermodynamic

Mustafa Can
Sakarya University, Vocational School of Arifiye,
Fatih Mah. Eşit Sok No. 7/A,
54580 Sakarya,
Turkey
E-mail: *mstfacan@gmail.com*

INTRODUCTION

Since the Neolithic period, organic and synthetic dyes have been used in a variety of different applications. When they mix with water, it is difficult to treat as the dyes have a synthetic origin and a complex molecular structure (Forgacs *et al.* 2004). Synthetic dyes exhibit considerable structural diversity, but they can be classified as azo, anthraquinone, sulfur, indigoid, triphenylmethyl (trityl), and phthalocyanine derivatives. However, it has to be emphasized that the overwhelming majority of synthetic dyes currently used in the industry are azo derivatives (Gupta & Suhas 2009).

Classification by application is the principal system adopted by the color index. A wide range of methods has been developed for the removal of synthetic dyes from waters and wastewaters to decrease their impact on the environment. The adsorption process is one of the most effective methods for removing dyes.

Several studies have been found in the literature that deal with the removal of metal complex dyes. (Vijaykumar *et al.* 2006; Aksu & Balibek 2010; Demirci *et al.* 2011; Deniz & Karaman 2011a, b; Du *et al.* 2012). Whereas, agricultural biosorbents have been used for the removal of dyes from aqueous solution (Deniz & Karaman 2011a, b; Sen Afroze & Ang 2011; Zhang *et al.* 2011; Choy & Gordon 2012). Among the untreated materials that have been investigated, many agricultural residues such as wheat straw, rice husk, corn cobs, and wood chips have been used successfully to adsorb individual dyes and dye mixtures in textile effluent (Ramakrishna & Viraraghavan 1997; Crini 2006; Can 2013a, b). However, only a limited number of studies have been carried out with sawdust (Sidiras *et al.* 2011; Hanafiah *et al.* 2012). Despite interesting adsorption capacities, to the best of our knowledge, nothing has been done with red pine sawdust covering equilibrium, kinetic and one step batch adsorber design of acid yellow 132 metal complex dye adsorption.

In the present research, untreated red pine sawdust (*Pinus resinosa*) was used as the biosorbent for the removal of acid yellow 132 dyes because *Pinus resinosa* is found abundantly in Turkey. The sorption of acid yellow 132 (AY132) at solid/liquid interfaces has been studied extensively under equilibrium conditions. We investigated the affecting parameters such as the dose of sawdust, particle size, pH, initial dye concentration, temperature and contact time. The Langmuir, Freundlich, Temkin, Dubinin–Radushkevich (D-R), and Redlich–Peterson (R-P) isotherms were used to match the equilibrium data. This paper also presents the thermodynamic parameters related to the adsorption of MG, such

doi: 10.2166/wst.2015.164

as Gibbs free energy change (ΔG°), enthalpy change (ΔH°) and entropy change (ΔS°), which have been calculated and discussed. Furthermore, the kinetics involved in the sorption process was evaluated at different initial acid yellow 132 concentrations by using four different kinetic equations (pseudo-first- and second-order, intraparticle diffusion and the Elovich equations). Kinetic parameters and Langmuir constants of experimental data were calculated using non-linear regression by means of Microsoft Excel's Solver Extension software program. The chi-square test was used as the determining parameter to evaluate the models that had the best fit with experimental data. Finally, Fourier transform infrared (FTIR) spectroscopy measurements were used for the designated adsorption mechanism of AY132.

METHODOLOGY

Materials

Turkish red pine sawdust was used in the present study as adsorbent and was supplied from a lumber mill in Sakarya, Turkey. The AY132 was obtained from Archroma Kimya (Gebze, Turkey). The charred sawdust was acid-hydrolyzed (0.5 MHCl) to remove sugars from the wood. To prevent hydrolysis of the adsorbent, it was washed with distilled water, and dried at 353 K for 12 hours. After drying, the rep pine sawdust was sieved using American Society for Testing and Materials standard sieves to obtain $\leq$53, 53–75, 75–90, 90–150, and 150–500 μm size fractions. The AY132 was obtained from Archroma (Gebze, Turkey). It was then used directly as adsorbent. All the chemicals were used as received without further purification or treatment and purchased from Merck in Darmstadt, Germany.

Batch adsorption studies

The effect of particle size distribution changing from $\leq$53, 53–75, 75–90, 90–150, and 150–500 μm range was studied. The pH of the dye solutions was adjusted with dilute HCl or NaOH solution by using a pH meter. At the same time, the effect of mixing speed was investigated by changing the speed between 200 and 600 rpm. To investigate the effect of adsorbent dosage, 0.5–3 g pine sawdust mass range was selected. To determine the thermodynamic parameters of adsorption, experiments were performed at different temperatures between 298 and 353 $\pm$ 2 °K. Dye solutions (1,000 mL) of 100 mg/L initial concentration were agitated with 1 g of the adsorbent on a mechanical stirrer for 3 hours. Five mL samples were centrifuged and the solutions were filtered through a filter paper to avoid any solid particles in the aqueous phase. Once maximum absorbance, λ_{max}, was determined, these values were used for analysis. The supernatant solution was analyzed for residual dye concentration using an ultraviolet–visible (UV–vis) light spectrophotometer (Shimadzu UV-150-02, Shimadzu Corp., Kyoto, Japan) at 428 nm for AY132 dye. The dye concentration was measured at the wavelength corresponding to maximum absorbance.

A volume of the AY132 dye solutions with concentrations ranging from 25 to 300 mg/L were placed in 1 L conical flasks. Optimum working pH was adjusted before biosorbent was added. An accurately weighed amount (1 g) of Turkish red pine tree sawdust was added to the solutions. The conical flasks were then agitated at a constant speed of 200 rpm in a water bath set at 298 $\pm$ 2 °K. Total contact time was selected as 180 minutes.

The samples were withdrawn from the stirrer at predetermined time intervals and the dye solution was separated from the adsorbent by centrifugation. The absorbance of supernatant solution was measured using the Beer–Lambert–Bouguer equation. Once maximum absorbance, λ_{max}, was determined, these values were used for analyzing. The supernatant solution was analyzed for residual dye concentration using a UV-vis spectrophotometer (Shimadzu UV-150-02, Shimadzu Corp., Kyoto, Japan) at 428 nm for the AY132 dye.

The point of zero charge of Turkish red pine tree sawdust was determined in order to understand the adsorption mechanism. The pH drift method was used to measure the pH at the potential of zero charge (pH_{zpc}) of Turkish red pine tree sawdust. The pH of a solution of 0.01 M potassium nitrate (KNO_3) was adjusted to between pH 2 and 12. Adsorbent (0.10 g) was added to 20 mL of the solution. After the pH had stabilized (typically after 24 hours), the final pH was recorded. The graphs of final versus initial pH were used to determine the points at which initial pH and final pH values were equal. This was taken as the point of zero charge.

Instrumentation

The field emission scanning electron microscope (FESEM) used in the study was a Quanta FEG 450 Field Emission Scanning Electron Microscope (FEI Company, Hillsboro, OR, USA). The FESEM and EDAX tests were carried out on samples operating at 10 kV and 20 kV, respectively, which were Au coated. The magnifications were from ×100 to ×100,000.

FTIR spectra were obtained using a spectroscope (Spectrum Two Spectrometer, PerkinElmer, Waltham, MA, USA).

Samples were analyzed in attenuated total reflectance mode using a ceramic light source, a KBr/Ge beam splitter and a deuterated l-alanine triglycine sulfate detector. The sampling technique used was diffuse reflectance. The powder samples were scanned for wavenumber 600–4,000 cm^{-1}.

RESULTS AND DISCUSSION

Effect of particle size

To understand the effect of the particle size on adsorption, five different particle sizes in the range (≤53, 53–75, 75–90, 90–150, and 150–500 μm) were studied and the results are provided in Figure 1. Optimum particle size ranges can be observed as 150–500 μm. In these size ranges, capacity was determined as 62 mg dye/g red pine sawdust for AY132. A decrease in the particle size would lead to an increase in surface area and an increase in the adsorption opportunity at the outer surface of the pine sawdust. In addition, adsorbed dye molecules onto external surfaces of the red pine sawdust may be subjected to diffusion from the external surface into the pores of the sawdust adsorbent. Furthermore, sawdust contains long capillary tube, which are longest at large particle sizes. Hereby, the surface area per mass could be optimal at this particle size. When the particle size of adsorbent is reduced the pore surface area and amount of adsorbent is reduced. This optimum value shows AY132 dye molecules having diffusion capacity into pores.

Effect of pH

The pH of the aqueous solution is one of the important controlling parameters in the sorption process of textile dyes, because H^+ themselves are competing with metal ions. The pH at the zero point of charge of Turkish red pine tree sawdust was found to be 6.3. The effect of pH can be explained in terms of pH_{zpc} of the adsorbent, at which the adsorbent is neutral. The surface charge of the red pine sawdust is positive when the media pH is below the pH_{zpc} value while it is negative at a pH over the pH_{zpc} (Shukla *et al.* 2002; Can 2015). The effect of pH was studied in the pH ranges of 2–11 and results are shown in Figure 2; as shown, the capacity increases significantly with a decrease in the pH. The maximum dye removals were observed at pH 2. At this pH value, the red pine sawdust surface charged positively, hence solution pH is below the pH_{zpc}. Even the molecular structure of dye is concealed, It can be said that the main carbon chain of acid yellow 132 dye is negatively charged. It is very likely that positively charged red pine sawdust particle surfaces would lead to electrostatically increased adsorption of acid dye anions. Another possibility is that with a decreasing pH, dyes charges are mainly neutral, hence it could be adsorbed by a hydrogen bonding mechanism along with ion exchange. Therefore, it seemed that the maximum adsorption capacity of AY132 on the adsorbents could be obtained at a pH near 2. With a decrease in pH from 11 to 2, the amounts of adsorbed dye for the AY132 increased from 46 mg/g to 66.6 mg/g, respectively.

As can be seen in Figure 2, the results showed that the maximum biosorption of AY132 was observed at pH 2 using 150–500 μm particle size of adsorbent. At lower pH values, the biosorption of dye was not effective. Besides, at lower pH, the adsorbent surface turned out to be positively charged and electrostatic attraction engaged between sawdust and AY132 dye. Furthermore, at basic pH, adsorption decreased due to the presence of hydroxyl ions, which competed with AY132 anions. As can be seen in Table 1, the pseudo-second-order model best describes the AY132 adsorption onto red pine sawdust. Other kinetic models that fit the experimental results, the Elovich equation,

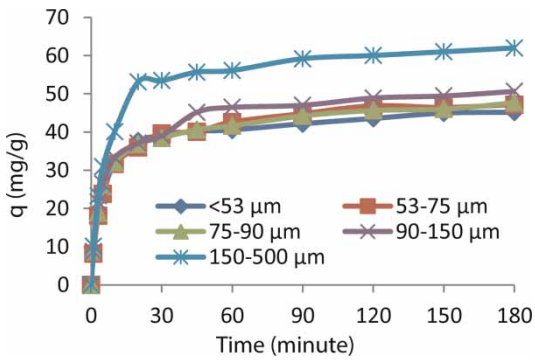

Figure 1 | The effects of biosorbent particle size on AY132 adsorption (pH: 6.3, C_0 = 100 mg L^{-1}, temperature: 298 °K, dose: 1 g/100 mL, stirring rate: 600 rpm).

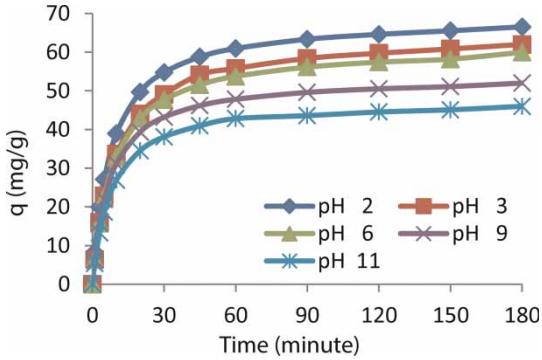

Figure 2 | The effects of pH on AY132 adsorption (C_0 = 100 mg L^{-1}, 298 °K, dose: 1 g/100 mL, stirring rate: 600 rpm, particle size: 150–500 μm).

pseudo-first-order equation, and intraparticle diffusion equation, respectively.

Effect of stirring rate

To understand the effect of stirring rates on the adsorption of AY132 dye onto red pine sawdust, experiments were carried out in batch systems with different stirring rates ranging from 300 to 600 rpm at pH 2 and using 150–500 μm particle size of adsorbent. The obtained results are shown in Figure 3.

It can be seen that the increase in stirring rate leads to a large increase in AY132 adsorption capacities, from 52.3 to 66.6 mg g^{-1}. This situation can be explained by the fact that with increasing stirring rates, mobility of the system normally increased. At the same time, it is expected that intraparticle diffusion speed increased; hence, the number of free active sites of the red pine sawdust particle were higher than at low rpms. This can be explained by external diffusional limitations, which are overcome for higher stirring rates. Moreover, although it is clear that the stirring rate impacts the adsorption kinetic rate, it is disputable that it will impact the adsorption capacity (at equilibrium). Moreover, dye molecules diffuse into capillary pores of the red pine sawdust. As a result, a 600 rpm stirring rate was selected for further experiments.

Effect of adsorbent dose

The effect of the adsorbent dosage on adsorptions of AY132 on red pine sawdust is shown in Figure 4. Red pine sawdust dosage was varied between 0.5 and 3 g/L using 100 mg/L initial dye concentration with particle size 150–500 μm at pH 2, 600 rpm stirring rate (Table 1). It can be seen from Figure 4 that the removal of dye increased with an increase in adsorbent dosage. The efficiency was 67 and 51% at the adsorbent concentration of 10 g/L, while it varied from 67 to 79%, at adsorbent concentrations of 10–30 g/L for AY132. Although there was a three-fold increase in adsorbent dosage, the removal greater than 10 g/L increased only up to about 10%.

By increasing the red pine sawdust dose, the amount of adsorbed dye increases, but adsorption and adsorption densities decrease. This is due to the number of available adsorption sites increasing by increasing the adsorbent dose. In addition, aggregation of particles may have a reductive impact on adsorption density. This situation will reduce the surface area of adsorbents and increase the diffusion path length. Thus, the equilibrium concentration is considered to be 10 g/L for red pine sawdust.

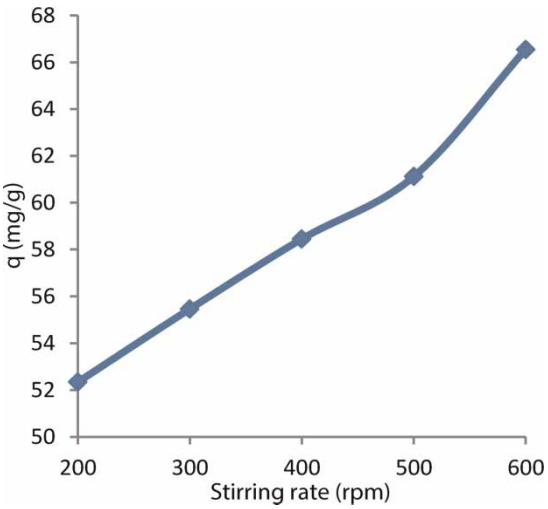

Figure 3 | The effects of stirring rate on AY132 adsorption ($C_0 = 100$ mg L^{-1}, 298 °K, dose: 1 g/100 mL, contact time: 180 minutes, pH = 2, particle size: 150–500 μm).

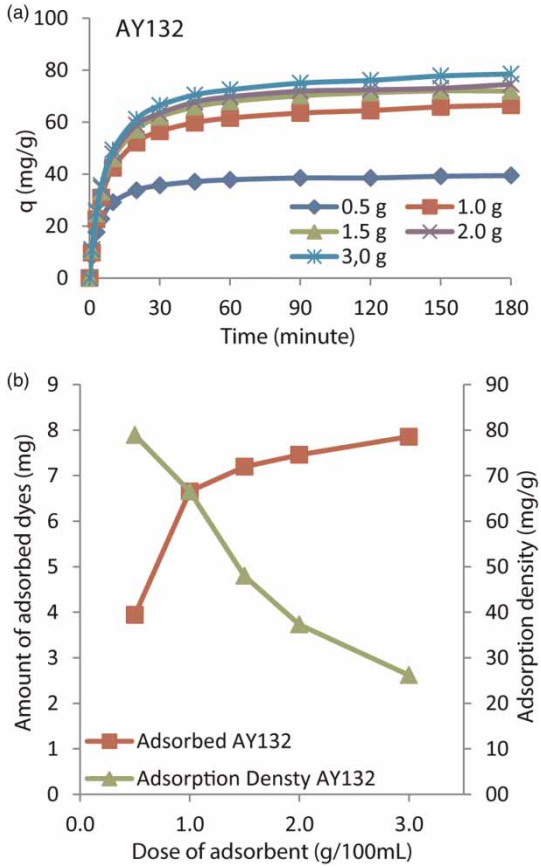

Figure 4 | The effects of sorbent dosage on AY132 adsorption (a) and adsorption density (b) ($C_0 = 100$ mg L^{-1}, 298 °K, contact time: 180 minutes, pH = 2, particle size: 150–500 μm, 600 rpm, 100 mL).

Table 1 | Kinetic parameters for the effects of sorbent particle size, pH, dose, and initial concentration on the sorption of AY132 onto red pine sawdust

		First-order kinetic equation				Second-order kinetic equation				The Elovich equation				Intraparticle diffusion equation		
Parameters	$q_{e,exp}$ (mg/g)	q_1 (mg/g)	k_1 (1/min)	r^2	x^2	q_2 (mg/g)	k_2 (g/(mg min.))	r^2	x^2	α (mg g^{-1} min^{-1})	β (mg g^{-1})	r^2	x^2	k_{int} (mg g^{-1} min.$^{-1/2}$)	r^2	x^2
≤53 μm	45.19	39.29	0.207	0.9720	2.540	45.19	0.0049	0.9971	0.2161	30.28	0.1341	0.9655	3.132	4.609	0.7336	49.80
53–75 μm	47.20	39.95	0.235	0.9360	5.556	46.91	0.0044	0.9946	0.3892	28.24	0.1321	0.9824	2.034	4.719	0.7801	45.67
75–90 μm	47.65	40.25	0.263	0.9350	5.160	46.11	0.0050	0.9930	0.4694	35.76	0.1381	0.9811	2.291	4.725	0.7677	48.72
90–150 μm	50.64	45.26	0.247	0.9227	7.444	49.34	0.0045	0.9875	1.0753	38.27	0.1229	0.9842	2.888	5.195	0.7823	49.60
150–500 μm	62.02	56.28	0.227	0.9522	6.970	62.81	0.0031	0.9969	0.3129	41.59	0.0969	0.9661	4.934	6.394	0.7443	63.74
pH 2	66.55	61.68	0.1114	0.9813	2.729	68.67	0.0019	0.9999	0.0260	20.68	0.0907	0.9810	2.206	6.731	0.8069	49.30
pH 3	59.98	57.32	0.0937	0.9830	2.364	64.54	0.0017	0.9998	0.0183	19.31	0.0862	0.9849	2.079	6.169	0.8310	37.97
pH 6	62.02	55.02	0.0969	0.9823	2.287	61.86	0.0018	0.9998	0.0212	18.99	0.0899	0.9848	1.954	5.943	0.8282	37.54
pH 9	52.01	48.31	0.1146	0.9829	1.821	53.76	0.0025	0.9999	0.0142	19.09	0.1038	0.9786	2.091	5.272	0.7968	40.29
pH 11	46.00	42.86	0.1081	0.9852	1.490	47.79	0.0027	0.9998	0.0181	16.24	0.1168	0.9776	1.974	4.649	0.7998	34.27
0.5 g	39.45	37.28	0.2003	0.9829	1.302	40.15	0.0066	0.9999	0.0049	32.41	0.0885	0.9458	37.30	4.155	0.6925	51.38
1.0 g	66.55	61.77	0.1360	0.9808	2.561	68.02	0.0024	0.9998	0.0167	29.80	0.0839	0.9749	3.075	6.819	0.7743	60.18
1.5 g	71.97	67.89	0.1326	0.9822	2.760	74.76	0.0022	0.9999	0.0133	32.20	0.0763	0.9733	3.506	7.467	0.7716	65.97
2.0 g	74.57	69.52	0.1348	0.9827	2.639	76.67	0.0021	0.9999	0.0153	33.15	0.0745	0.9721	3.816	7.650	0.7678	68.52
3.0 g	78.55	72.96	0.1294	0.9816	2.931	80.39	0.0020	0.9999	0.0174	33.20	0.0704	0.9759	3.504	8.029	0.7807	68.07
25 mg/L	17.55	16.23	0.4888	0.9793	0.450	16.99	0.0438	0.9967	0.0668	17.55	0.1142	0.7898	120.0	1.841	0.5264	35.19
50 mg/L	35.06	33.86	0.2803	0.9844	0.998	36.00	0.0109	0.9997	0.0161	35.06	0.1726	0.9251	4.730	3.781	0.6110	59.22
100 mg/L	66.55	61.89	0.1353	0.9818	2.455	68.01	0.0025	0.9999	0.0136	29.66	0.0837	0.9739	3.196	6.823	0.7723	60.42
200 mg/L	130.8	120.8	0.0934	0.9821	5.044	136.3	0.0008	0.9998	0.0595	40.31	0.0408	0.9856	4.387	13.01	0.8332	79.12
300 mg/L	190.4	179.8	0.1279	0.9831	6.623	198.6	0.0008	0.9999	0.0463	79.82	0.0284	0.9731	9.597	19.71	0.7740	169.8

Effect of contact time and initial dye concentration

The preliminary experiments showed that the adsorption of AY132 is fast at the initial stages and becomes slower near the equilibrium. This is valid for all mass transfer processes, as the driving force is the highest at time zero. Figure 5 presents the plots of the AY132 removal versus contact time for red pine sawdust at initial concentrations between 25 and 300 mg/L, at 298 K, with a contact time of 180 minutes, with particle size 150–500 μm, at pH 2, and a 600 rpm stirring rate. The rate of dye removal is very rapid during the initial 3 minutes and the plot flattens thereafter, as can be seen from Figure 5 for AY132 dye. It can be seen that there was no considerable change for removal of AY132 after 120 minutes of contact time for different initial concentrations. Figure 5 shows that for lower initial dye concentration, the time needed to reach equilibrium is lower.

Adsorption kinetics

Kinetic studies for 100 mg/L initial dye concentration were carried out at 25 °C and the experimental data are illustrated in Figure 6. Table 1 lists parameters calculated from these four models and their chi-square (x^2) and correlation coefficients (r^2) values. The non-linear regression is a suitable method for applying kinetic models; here, the chi-square error function is eligible to determine the connection between measured and modeled values. However, the correlation coefficients were (r^2) used as a complementary error function. The pseudo-second-order model provides low x^2 values, which suggested that the AY132 adsorption process is a second-order rate. The maximum deviation was observed as 4% at a 300 mg/L initial concentration of AY132 dye.

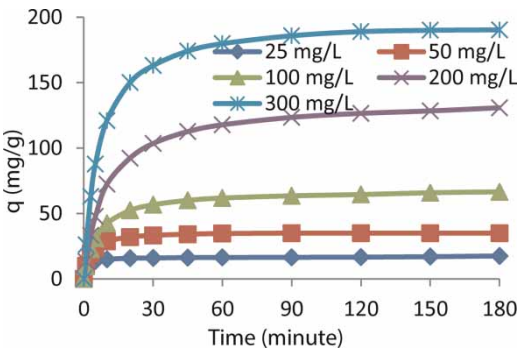

Figure 5 | The effects of initial dye concentration on AY132 dye sorption (298 °K, pH = 2, particle size: 150–500 μm, 600 rpm, 1 g of sorbent).

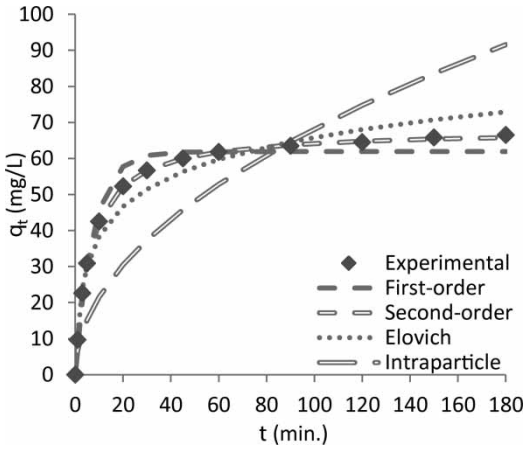

Figure 6 | The measured and non-linear modeled time profiles for biosorption of AY132 dye at 100 mg/L initial dye concentration onto red pine sawdust at a temperature of 298 °K.

It can be revealed that the AY132 adsorption process onto red pine sawdust was a rate-controlled process, based on the assumption that the rate limiting step may include chemical absorption involving valence forces through sharing or exchange of electrons between adsorbent and adsorbate. Indeed, the sorption of any dyes from the aqueous phase onto the solid phase is a multi-step process involving transport of dye from the aqueous phase to the surface of the adsorbent particles (external diffusion) and then, diffusion of dye via the boundary layer to the surface of the solid particles (surface diffusion) followed by transport of dye from the solid particle's surface to its interior pores (intraparticle diffusion), which is likely to be a slow process (Dabrowski 2001). But it can be revealed from experimental results that sorption of AY132 dye at an active site on the red pine sawdust surface could mostly occur and be called chemical a reaction such as ion-exchange, complexation and chelation. AY132 dye sorption is controlled usually by either intraparticle or surface diffusion because the cell walls of sawdust mainly consist of cellulose and lignin, and many hydroxyl groups, such as tannins or other phenolic compounds (Can *et al.* 2013). Similar results have also been observed with BB69, AB25, methylene blue, Bismarck brown, and acridine orange dyes onto wood (Ho & McKay 1998; Hamdaoui 2006). The intraparticle equations do not give a good fit to the experimental data for the sorption of AY132 dye.

Adsorption isotherms

Several isotherm equations are available and four important isotherms were selected in this study, namely the Langmuir,

Freundlich, Tempkin, D-R, and R-P isotherms. In this study, a comparison of a non-linear and two linear solutions of the Langmuir isotherm were carried out first. Then, Freundlich, Tempkin, D-R, and R-P were applied to the experiment of two dyes' sorption on red pine sawdust. Here, at linear forms, Pearson's correlation coefficient (r^2) error function and at non-linear solutions, Pearson's chi-squared (x^2) error function were taken into consideration, then for others, the error function was calculated. In addition, in the non-linear Langmuir solution, where the predicted values generated from a model are different from linear regression, an r^2 value can be calculated between the measured q_e and modeled q_e data values. In this case, the value is not directly a measure of how good the modeled values are, but rather a measure of how good a predictor might be when constructed from the modeled values. This usage is specifically the definition of the term 'coefficient of determination': the square of the correlation between two variables.

The chi-squared distribution value of the D-R isotherm was significantly higher than each value for AY132 dye adsorption onto red pine sawdust. Based on the x^2 values, as indicated in Table 2, it can be said that the non-linear method is the most reliable method for solution of the Langmuir isotherm. Beyond that, the best fitting isotherm of the five studied isotherms is the R-P isotherm for AY132 adsorption. The coefficient of determination (r^2) was able to point to the Langmuir non-linear method as the most appropriate (having r^2 0.9996 value). Because the R-P isotherm's β value is equal to 0.9999, the most reliable Langmuir isotherm solution is non-linear regression. These confirm the monolayer coverage of dyes onto red pine sawdust particles, and also the homogeneous distribution of active sites on the adsorbent since the Langmuir equation assumes that the surface is homogeneous. According to the Langmuir non-linear method, the monolayer saturation capacity of AY132 dye onto red pine sawdust was determined as 79.50.

The calculated R_L values at different initial dye concentrations are shown in Figure 7. Dimensionless constant, R_L, indicates the shape of the isotherms to be either unfavorable ($R_L > 1$), linear ($R_L = 1$), favorable ($0 < R_L < 1$) or irreversible ($R_L = 0$). It was observed that R_L values were determined between 0.9339 and 0.5408 for AY132 dye. This indicated that adsorptions were more favorable for the higher initial dye concentrations than for the lower ones.

Langmuir isotherm constants, r^2, and x^2 values are listed in supporting information in Table 2. Freundlich isotherm is widely applied in heterogeneous systems, especially for organic compounds or highly interactive species on activated carbon and molecular sieves. The slope ($1/n$) ranges between 0 and 1 and is a measure of adsorption intensity or surface heterogeneity, and it becomes more homogeneous when its value gets closer to one. Slopes of the AY132 dye were determined as 0.8789. These results are further evidence of the surface homogeneity. The Tempkin isotherm shows less agreement with the experimental data, with x^2 values of 3.772 for AY132; hence, it can be considered as an indication of the surface not being heterogeneous. Here, initial concentrations having relatively high values (Table 2 Langmuir's R_L values) caused relatively low x^2 values for all two dye adsorption systems.

The D-R isotherm constant, β (mmol^2/J^2), has been used to calculate the mean free energy (E) of sorption per mole of the adsorbate. The E value was calculated as 1.524 for the AY132 dye. Because of E in the range of $8 < E < 16$ kJ/mol, adsorption is governed by an ion-exchange mechanism (Özcan *et al.* 2005). Using Langmuir's Qmax (mg/g) and

Table 2 | Langmuir isotherm constants for AY132 dye adsorption onto red pine sawdust

Isotherm	K_L (L/g)	a_L (L/mg)	Q_{max} (mg/g)	R_L	r^2	x^2
Lineweaver-Burk linear	0.2448	0.0048	50.97	0.8928–0.4097	0.9991	0.1621
Langmuir linear	0.2347	0.0035	66.28	0.9187–0.4849	0.8795	0.0688
Non-linear regression	0.2249	0.0028	79.50	0.9339–0.5408	0.998*	0.0553
Freundlich	K_f (L/g)	n			r^2	x^2
	3.232	1.138			0.9988	0.2170
Tempkin	A (L/g)	B (j/mol)			r^2	x^2
	0.1303	6.064			0.8984	3.772
D-R	β (mmol/j)^2	q_m (mmol/g)	E (kJ/mol)		r^2	x^2
	0.2154	10.66	1.524		0.7661	51.71
R-P	K (L/g)	a (L/mg)	β		r^2*	x^2
	0.2249	0.0028	0.9999		0.9913	0.0062

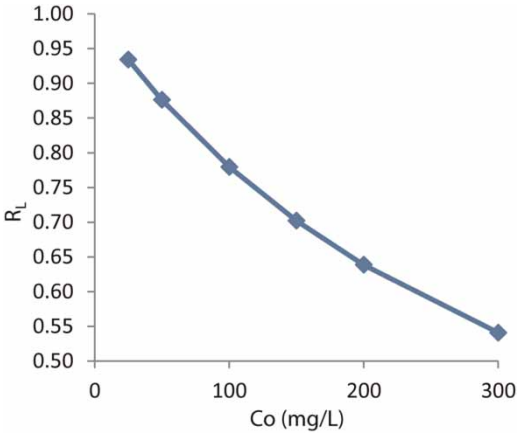

Figure 7 | Plots of separation factor versus initial dye concentrations.

D-R's qm (mmol/g) values, the unknown molecular weight of dyes can be calculated approximately. The reason is that, especially with the D-R isotherm, the compliance of isotherms with experimental data is low. The molecular weight of dye was calculated as ~7,457.8 for AY132. The R-P isotherm parameters $K(\mathrm{L/g})$, $a\left(\mathrm{L/mg^{1-1/A}}\right)$, and β can be seen in Table 2. Because of isotherm unitless constant β values having 0.9999 and $= 1$ for each adsorption system, the adsorption isotherm fits the Langmuir isotherm.

A comparison is also made between the experimental data and worked isotherms plotted in Figure 8. Using supporting information in Table 2, the Langmuir, Freundlich, and R-P isotherms generated a satisfactory fit to the experimental data in each dye adsorption system. Despite D-R isotherm representing adsorption systems at low concentrations, the Tempkin isotherm was generally in more agreement with the experimental data than the D-R isotherm. Based on Figure 8, it can be said that the R-P isotherm generated a satisfactory fit with the experimental data in all data points.

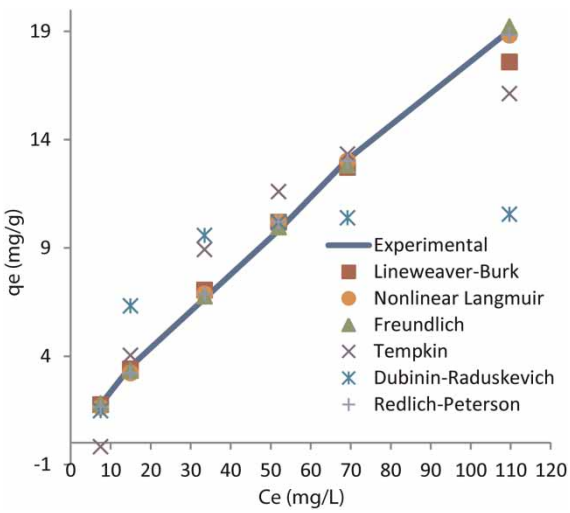

Figure 8 | Equilibrium curves for adsorption of AY132 onto red pine sawdust ($C_0 = 25$–300 mg L^{-1}, 298 °K, 180 minutes., pH = 2, 150–500 μm particle size, 600 rpm, 100 mL, 1 g adsorbent).

Effect of temperature on adsorption

To discuss the effect of temperature on adsorption of AY132 dye onto red pine sawdust, experiments were conducted at temperatures of 298, 313, 333, and 353 °K, and the results are shown in Figure 9. As shown in Figure 9, the results indicate that each amount of adsorbed dye decreases with an increase in temperature. For example, for an initial AY132 dye concentration of 100 mg/L, when increasing initial solution temperature from 298 to 353 °K, the amount of dye adsorbed per unit weight of red pine sawdust decreases from 66.21 to 38.88 mg/L. The decrease in the adsorption capacity at increased temperatures indicates the exothermic nature of the adsorption process of AY132 dye onto red pine sawdust.

Determination of thermodynamic parameters

The plot of $\ln K_L$ against $1/T$ (in Kelvin) should be linear, from which ΔH° and ΔS° were calculated from the slope and intercept, respectively. The slope of the Van 't Hoff plot is equal to $-\Delta H^0/R$, and its interception is equal to $\Delta S^0/R$ from Equation (10). The Van 't Hoff plot for the adsorption of dyes onto red pine sawdust is given in Figure 10. Obtained thermodynamic parameters are given in Table 3, and the negative values of ΔG^0 at different temperatures indicate the spontaneous nature of the adsorption process.

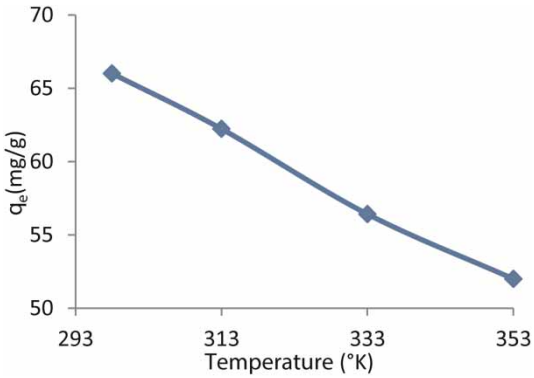

Figure 9 | Effect of temperature on AY132 dye adsorption. ($C_0 = 100$ mg L^{-1}, 180 minutes, pH = 2, 150–500 μm particle size, 600 rpm, 100 mL, 1 g adsorbent).

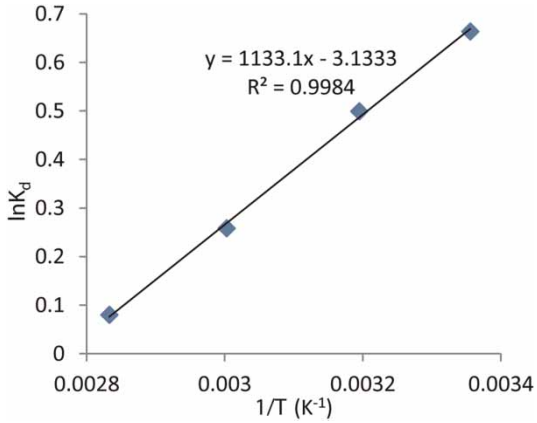

Figure 10 | Van 't Hoff plot of $\ln K_d$ versus $1/T$ for the estimation of thermodynamic parameters.

The negative value of ΔH° suggests the exothermic nature of each adsorption system. Generally, when the ΔH^0 value is smaller than 40 kJ/(mol K), this interaction is assumed as a weak interaction or physisorption (Yao *et al.* 2010). Based on this study, ΔH^0 values were determined as −9.420 kJ/(mol K) for AY132, and this suggests that the adsorption of dyes onto red pine sawdust was a physisorption process. The negative value of ΔS^0 suggests the decreased randomness at the solid/solution interface during the adsorption of AY132 dye red pine sawdust. As is well known, all systems move toward minimum energy and maximum randomness. Here, for these dye systems, although randomness has decreased, the tendencies of systems toward minimum energy seem to be dominant.

Characterization

The FTIR spectra of red pine sawdust and A132 adsorbed red pine sawdust are illustrated in Figure 11. The cell walls of pine sawdust mainly consist of cellulose, hemicelluloses, lignin and many hydroxyl groups, such as tannins or other phenolic compounds (Can 2013a, b). Lignin is a polymer material built up from the phenyl propane nucleus, an aromatic ring with a three-carbon side chain. Vanillin and syringaldehyde are the two other basic structural units of lignin molecules. Tannins are complex polyhydric phenols, which are soluble in water and have the property of precipitating protein (gelatin).

The comparison of the FTIR spectra shows that some peaks were shifted. In the case of the red pine sawdust, there is a strong peak at wavenumber 3,338 cm^{-1} representing the single —OH stretching of the phenol group of cellulose and lignin, and the peak at 2,886 cm – 1 indicates the presence of single —CH_2 stretching of the aliphatic compound. The peaks that resemble a saw around 2,000 cm^{-1} indicate the presence of single —NH stretching. The appearance of peaks at 1,713 cm^{-1} and 1,656 cm^{-1} indicate the presence of C = O stretching of the aldehyde group and C = C stretching of the phenol group, respectively. Whereas the peaks at 1,590 cm^{-1} and 1,507 cm^{-1} in the spectrum of red pine sawdust can be due to C = C of the benzene aromatic ring, peaks at 1,453 cm^{-1} and 1,422 cm^{-1} can be due to single —CH_2 bending and single —OH bending, respectively. The peaks at 1,397 and 1,315 cm^{-1} show C—O—H bending and C—H in plane deformation. Peaks at 1,266 cm^{-1} and 1,157 cm^{-1} in the FTIR spectrum of sawdust can be due to C—O stretching of the phenolic group and the six-member cyclic ether group of cellulose, respectively. These wavenumber values are very close to those reported for pine sawdust by (Sidiras *et al.* 2011).

After adsorption of AY132, the peak at 1,695 cm^{-1} appeared, which indicated the presence of the carboxylic acid group since the AY132 solution was acidic. The interaction between AY132 and the carboxylic, amino and hydroxyl groups was detected by the shift in wavenumber from 3,338 to 3,875 cm^{-1}. The peak in sawdust at 1,157 cm^{-1} that also represented the C—N bending vibration had shifted to 1,187 cm^{-1} after AY132 adsorption. All the findings from FTIR spectra led to the conclusion that O and N-containing groups are the main adsorption sites for AY132.

The FESEM images at ×100,000 magnification of AY132 adsorbed red pine sawdust and at ×1,000 magnification of red pine sawdust are shown in Figure 12. The micrograph of AY132 adsorbed red pine sawdust particles (Figure 12(a)) reveals low porosity and irregular surface structure. Red pine sawdust has a macroporous structure due to the presence of large pores (Figure 12(b)).

Table 3 | Thermodynamic parameters for adsorption of AY132 dye onto red pine sawdust

		ΔG° (kJ/mol K)			
ΔH° (kJ/mol)	ΔS° (J/mol K)	298 °K	313 °K	333 °K	353 °K
− 9.420	− 26.05	− 1,644.46	− 1,299.38	− 714.91	− 234.91

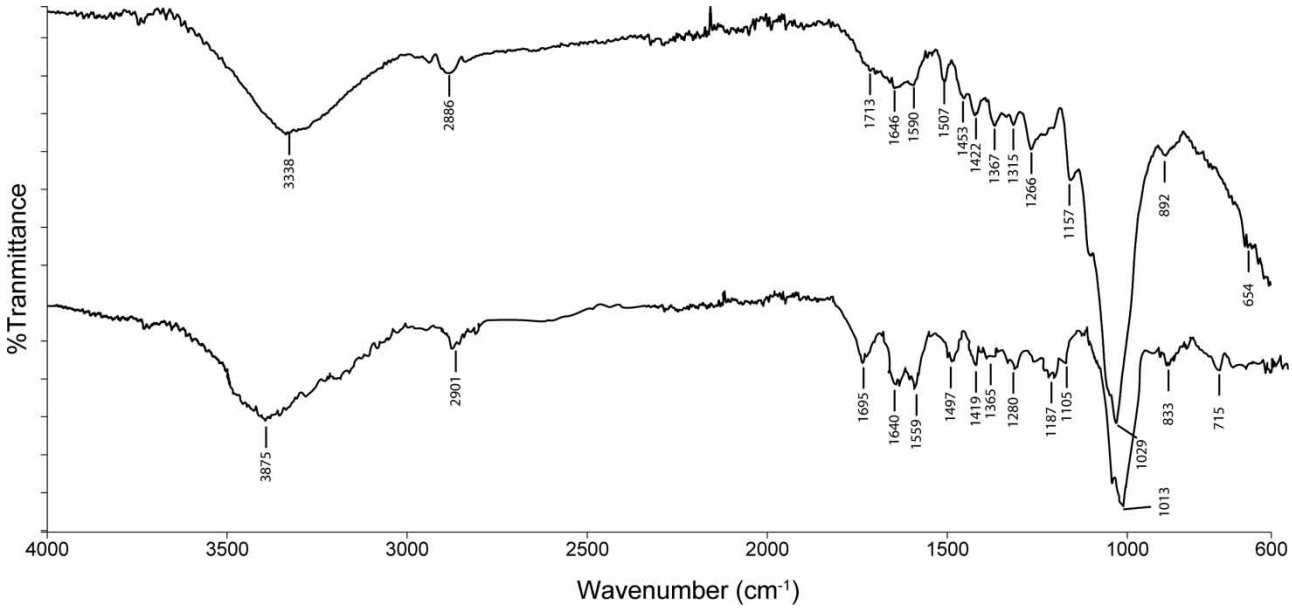

Figure 11 | FTIR spectra of sawdust and AY132 adsorbed sawdust.

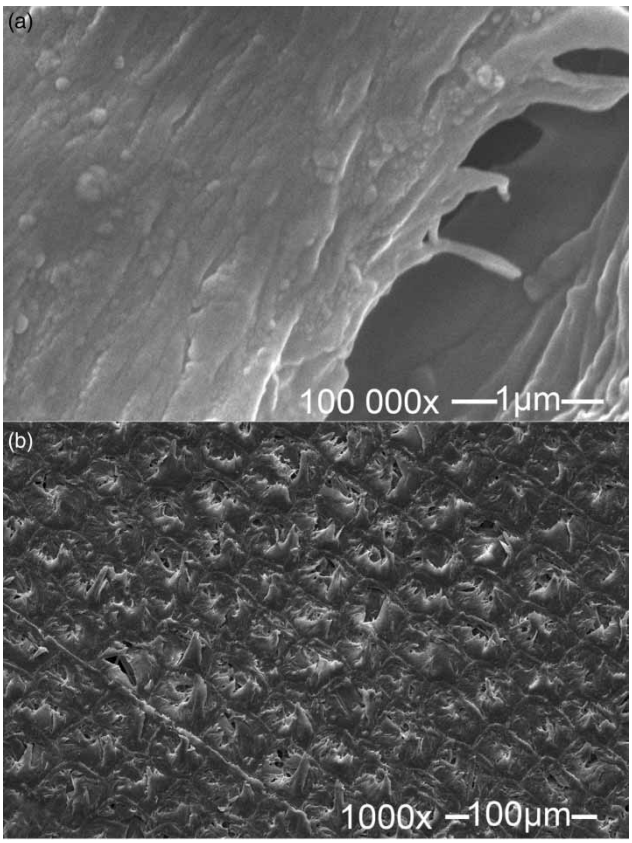

Figure 12 | FESEM micrograph of AY132 adsorbed (a) and natural (b) red pine sawdust particles (10 kV).

CONCLUSIONS

The future development of adsorption science represents a major challenge to industry and environmental fields because it is low cost. A low-cost biosorbent, red pine (*Pinus resinosa*) sawdust was used for removal of AY132 dye from aqueous solution in batch mode. The biosorption isotherm, thermodynamic and kinetic of red pine sawdust for each dye were investigated as a function of particle size, initial pH, stirring range, adsorbent dose, contact time, and initial dye amount.

The adsorbed amounts of dyes increased with increase in contact time. There was no considerable change for removal of AY132 dye after 120 minutes of contact time for different initial concentrations. It can be said that the equilibrium times are independent of each initial dye concentration.

The pseudo-second-order kinetic model supplied the best coherence with experimental data for each parameter. The monolayer sorption capacity of the biosorbent for AY132 dye was found as 79.50 mg g^{-1}. The thermodynamic studies indicated that the sorption processes were favorable, exothermic and minimum energy tendency driven. The randomness decreased at the solid/solution interface. Activation energies showed that AY132 dye adsorption onto the red pine sawdust was physical sorption. As a

result, red pine sawdust can be used as a low-cost adsorbent instead of more costly commercial adsorbents.

ACKNOWLEDGEMENT

The author declares that he has no financial interests.

REFERENCES

Aksu, Z. & Balibek, E. 2010 Effect of salinity on metal-complex dye biosorption by *Rhizopus arrhizus*. *Journal of Environmental Management* **91** (7), 1546–1555.

Can, M. 2013a Biomaterials derived from renewable resources for the recovery of precious metals. *Research Journal of Chemistry and Environment* **17** (12), 117–128.

Can, M. 2013b Vibrational Spectroscopy of Pyrogallol with a glance on the problems of formation of a Dimer. *Research Journal of Chemistry and Environment* **17** (12), 117–128.

Can, M. 2015 Investigation of the factors affecting acid blue 256 adsorption from aqueous solutions onto red pine sawdust: equilibrium, kinetics, process design and spectroscopic analysis. *Desalination and Water Treatment*. DOI: http://dx.doi.org/10.1080/19443994.2014.1003974.

Can, M., Emrah, B., Ahmet, Ö. & Mahmut, Ö. 2013 Synthesis and characterization of valonea tannin resin and its interaction with palladium (II), rhodium (III) chloro complexes. *Chemical Engineering Journal* **221**, 146–158.

Choy, K. K. H. & Gordon, M. 2012 Synergistic multilayer adsorption for low concentration dyestuffs by biomass. *Chinese Journal of Chemical Engineering* **20** (3), 560–566.

Crini, G. 2006 Non-conventional low-cost adsorbents for dye removal: a review. *Bioresource Technology* **97** (9), 1061–1085.

Dabrowski, A. 2001 Adsorption – from theory to practice. *Advances in Colloid and Interface Science* **93** (1–3), 135–224.

Demirci, A., Mutlu, M. B., Güven, A., Korcan, E. & Güven, K. 2011 Decolorization of textile azo-metal complex dyes by a halophilic bacterium isolated from Çamaltı Saltern in Turkey. *Clean – Soil, Air, Water* **39** (2), 177–184.

Deniz, F. & Karaman, Ş. 2011a Removal of an azo-metal complex textile dye from colored aqueous solutions using an agro-residue. *Microchemical Journal* **99** (2), 296–302.

Deniz, F. & Karaman, Ş. 2011b Removal of basic red 46 dye from aqueous solution by pine tree leaves. *Chemical Engineering Journal* **170** (1), 67–74.

Du, L.-N., Wang, B., Li, G., Wang, S., Crowley, D. E. & Zhao, Y.-H. 2012 Biosorption of the metal-complex dye Acid Black 172 by live and heat-treated biomass of *Pseudomonas* sp. strain DY1: kinetics and sorption mechanisms. *Journal of Hazardous Materials* **205–206**, 47–54.

Forgacs, E., Cserháti, T. & Oros, G. 2004 Removal of synthetic dyes from wastewaters: a review. *Environment International* **30** (7), 953–971.

Gupta, V. K. & Suhas, 2009 Application of low-cost adsorbents for dye removal – a review. *Journal of Environmental Management* **90** (8), 2313–2342.

Hamdaoui, O. 2006 Batch study of liquid-phase adsorption of methylene blue using cedar sawdust and crushed brick. *Journal of Hazardous Materials* **135** (1–3), 264–273.

Hanafiah, M. A. K. M., Ngah, W. S. W., Zolkafly, S. H., Teong, L. C. & Majid, Z. A. A. 2012 Acid Blue 25 adsorption on base treated *Shorea dasyphylla* sawdust: kinetic, isotherm, thermodynamic and spectroscopic analysis. *Journal of Environmental Sciences* **24** (2), 261–268.

Ho, Y. S. & McKay, G. 1998 Kinetic models for the sorption of dye from aqueous solution by wood. *Process Safety and Environmental Protection* **76** (2), 183–191.

Özcan, A. S., Erdem, B. & Özcan, A. 2005 Adsorption of Acid Blue 193 from aqueous solutions onto BTMA-bentonite. *Colloids and Surfaces A: Physicochemical and Engineering Aspects* **266** (1–3), 73–81.

Ramakrishna, K. R. & Viraraghavan, T. 1997 Dye removal using low cost adsorbents. *Water Science and Technology* **36** (2–3), 189–196.

Sen, Tushar K., Afroze, S. & Ang, H. M. 2011 Equilibrium, kinetics and mechanism of removal of methylene blue from aqueous solution by adsorption onto pine cone biomass of pinus radiata. *Water, Air, & Soil Pollution* **218** (1–4), 499–515.

Shukla, Alka, Zhang, Y.-H., Dubey, P., Margrave, J. L. & Shukla, S. S. 2002 The role of sawdust in the removal of unwanted materials from water. *Journal of Hazardous Materials* **95** (1–2), 137–152.

Sidiras, D., Batzias, F., Schroeder, E., Ranjan, R. & Tsapatsis, M. 2011 Dye adsorption on autohydrolyzed pine sawdust in batch and fixed-bed systems. *Chemical Engineering Journal* **171** (3), 883–896.

Vijaykumar, M. H., Veeranagouda, Y., Neelakanteshwar, K. & Karegoudar, T. B. 2006 Decolorization of 1:2 metal complex dye acid blue 193 by a newly isolated fungus, *Cladosporium cladosporioides*. *World Journal of Microbiology & Biotechnology* **22** (2), 157–162.

Yao, Y., Xu, F., Chen, M., Xu, Z. & Zhu, Z. 2010 Adsorption behavior of methylene blue on carbon nanotubes. *Bioresource Technology* **101** (9), 3040–3046.

Zhang, H., Tang, Y., Liu, X., Ke, Z., Su, X., Cai, D., Wang, X., Liu, Y., Huang, Q. & Yu, Z. 2011 Improved adsorptive capacity of pine wood decayed by fungi *Poria cocos* for removal of malachite green from aqueous solutions. *Desalination* **274** (1–3), 97–104.

First received 18 January 2015; accepted in revised form 23 March 2015. Available online 10 April 2015